



# Core-shell-like Ni-Pd nanoparticles supported on carbon black as a magnetically separable catalyst for green Suzuki-Miyaura coupling reactions



Jiawei Xia <sup>a,b</sup>, Yongsheng Fu <sup>a,\*</sup>, Guangyu He <sup>b</sup>, Xiaoqiang Sun <sup>b,\*</sup>, Xin Wang <sup>a,\*</sup>

<sup>a</sup> Key Laboratory of Soft Chemistry and Functional Materials, Nanjing University of Science and Technology, Ministry of Education, Nanjing 210094, China

<sup>b</sup> Key Laboratory of Fine Petrochemical Engineering, Changzhou University, Changzhou 213164, China

## ARTICLE INFO

### Article history:

Received 18 April 2016

Received in revised form 27 May 2016

Accepted 27 June 2016

Available online 28 June 2016

### Keywords:

Suzuki-Miyaura coupling reaction

Carbon black

Core-shell-like Ni-Pd nanoparticles

Mild conditions

## ABSTRACT

A magnetically separable core-shell-like catalyst Ni-Pd/CB is designed and synthesized via a facile sequential reduction strategy. It is found that the Pd nanocrystals with a thickness of ~1.67 nm and a length of ~7.92 nm are intimately coupled with the Ni cores and the formed core-shell-like Ni-Pd nanoparticles are well dispersed on the CB surface with much smaller particle size and narrower size distribution as compared with that of unsupported ones. The ligand-free Ni-Pd/CB nanocatalyst is evaluated for Suzuki-Miyaura coupling reaction and exhibits excellent catalytic activity under mild aerobic conditions without using toxic solvents and inert protective atmosphere, achieving green catalysis. The high catalytic performance of Ni-Pd/CB catalyst can be attributed to its unique core-shell-like nanostructure and the concerted effects between the individual components. The introduction of Ni not only makes the catalyst magnetically separable in a suspension system, but also significantly lowers the cost.

© 2016 Elsevier B.V. All rights reserved.

## 1. Introduction

As a palladium-catalyzed process, the Suzuki-Miyaura coupling (SMC) reaction has become one of the most useful and popular carbon–carbon bond-forming reactions due to its tolerance of a broad range of functional groups and its non-toxic by-products. Therefore, the SMC reaction has been widely used in organic synthesis of natural and non-natural products as well as bioactive compounds in the past few decades [1–6]. In the early stage, the SMC reaction was often performed in homogeneous alkaline systems using palladium-based complexes as the catalysts [4,7,8]. Until the end of 20th century, the triarylphosphine ligand-based catalysts were widely used for the SMC reaction [7]. After that, new bulky and electron-rich phosphine ligands were employed, as a result, the efficiency and selectivity of the reactions could be greatly improved, even in the ambient environment [1,7,8]. However, homogeneous catalytic systems suffer from various problems, such as using toxic solvents and needing complicated post-processing procedures due to the well soluble Pd complexes and ligands, which may have the

potential impact on the quality of both the product and environment, especially in pharmaceutical applications [2,9,10].

In recent years, the SMC reaction is being increasingly carried out with ligand-free Pd catalysts in heterogeneous systems without using protective atmosphere and toxic solvents [11–16]. Moreover, supported Pd nanoparticles have been developed as recyclable and efficient catalysts for the SMC reaction, which facilitates separation of the catalyst from the reaction products and reuse in succession [17–21]. It should be noted that Pd is a precious metal of low earth abundance and high cost, and therefore it is essential to replace or reduce the Pd dosage to overcome these disadvantages. One of the most effective ways is to create less expensive alloys or core-shell structures that mix Pd with nonprecious metals [22–27]. It is found that the synergistic effect between the different metals may lead to exceptional catalytic performance by inducing an extra electric field to facilitate electron transport [26,28,29], tuning the bonding pattern of the reactants and stabilizing the intermediates on the catalyst surface [30]. Another alternative approach to achieve a high Pd utilization is increasing the specific surface area by highly dispersing Pd nanoparticles on carbon supports with high surface areas. Among various carbon supports, Vulcan XC-72R carbon black (CB) is a widely used catalyst support due to its large surface area, high electrical conductivity, suitable pore structure, high availability and relatively low cost [31–33]. Nevertheless, there are some disadvantages of carbon black when used as catalyst support, for

\* Corresponding authors.

E-mail addresses: [fuyongsheng0925@163.com](mailto:fuyongsheng0925@163.com) (Y. Fu), [xqsun@cczu.edu.cn](mailto:xqsun@cczu.edu.cn) (X. Sun), [wangx@njust.edu.cn](mailto:wangx@njust.edu.cn) (X. Wang).

example, intrinsic CB only has limited oxygen-containing groups, which makes CB hydrophobic and is unable to provide enough anchoring sites for metal ions. It is reported that proper surface modification, such as acidification, can effectively produce plenty of oxygen-containing groups, leading to enhanced performance of CB supported catalysts [34].

Herein, we demonstrate a facile sequential reduction strategy to fabricate a Ni-Pd/CB catalyst for SMC reaction. TEM observation reveals clearly that the Pd nanocrystals with a thickness of ~1.67 nm and a length of 7.92 nm are intimately coupled with the Ni nano-cores and the resulting core-shell-like Ni-Pd particles are well dispersed on the CB surface with much smaller particle size and narrower size distribution as compared with that of unsupported ones. Encouragingly, the as-prepared Ni-Pd/CB catalyst exhibited superior catalytic activity in SMC reaction under mild conditions without using toxic solvents, ligands or inert protective atmosphere, achieving an efficient and green organic synthesis. Moreover, the presence of Ni element not only endows the catalyst with magnetically separable ability from a suspension system, but also significantly lowers the cost.

## 2. Experimental

### 2.1. Materials

Hydrazine hydrate ( $\text{N}_2\text{H}_4 \cdot \text{H}_2\text{O}$ , 80%), phenylboronic acid (97%), bromobenzene (99%) were all supplied by Aladdin Industrial Cooperation. Ethylene glycol (EG, 99.0%), nitric acid ( $\text{HNO}_3$ , 65–68%), nickel chloride ( $\text{NiCl}_2 \cdot 6\text{H}_2\text{O}$ , 98%), ethanol (EtOH), potassium carbonate ( $\text{K}_2\text{CO}_3$ ) were of analytical grade and purchased from Sinopharm Chemical Reagent Co., Ltd. XC-72 carbon black (CB) was obtained from Cabot Corporation. Potassium tetrachloropalladate ( $\text{K}_2\text{PdCl}_4$ , 99.99%) was bought from Alfa Aesar. All Chemicals were used without further purification and deionized water was used throughout the experiments.

### 2.2. Catalyst preparation

XC-72 carbon black was acidized with concentrate nitric acid according to the procedure as we reported previously [34]. The experiment procedure for the synthesis of Ni/CB is as follows: 0.30 g of CB was dispersed in 300 mL of EG and then heated to 60 °C under continuously mechanical stirring. 50 mL of EG solution containing 0.304 g of  $\text{NiCl}_2 \cdot \text{H}_2\text{O}$  was then added into the suspension dropwise. After 30 min of stirring, 25 mL of hydrazine hydrate (80%) and 20 mL of NaOH/EG (1 mol L<sup>-1</sup>) were injected into the above mixture, respectively. The reaction was maintained for 30 min and the resulting suspension was centrifuged, washed with deionized water and ethanol several times and finally freeze-dried. Then 20 mL of  $\text{K}_2\text{PdCl}_4$  (4.09 mg) solution was injected into the suspension of Ni/CB/H<sub>2</sub>O (25 mg/50 mL) and the mixture was kept stirring overnight. The catalyst was washed and dried subsequently, labeled as  $\text{Ni}_{0.20}\text{Pd}_{0.05}/\text{CB}$  (the subscripts represent the raw material feed rate of metals). Moreover,  $\text{Ni}_{0.10}\text{Pd}_{0.05}/\text{CB}$  and  $\text{Ni}_{0.30}\text{Pd}_{0.05}/\text{CB}$  were also synthesized for comparison under the same conditions.

### 2.3. Characterization

Morphology and structure of the catalyst were characterized by transmission electron microscope (TEM, JEOL JEM-2100, 200 kV) and powder X-ray diffraction (XRD, Bruker D8 Advanced diffractometer, Cu K $\alpha$ ,  $\lambda = 0.15406$  nm) with the scanning angle ranged from 10° to 80° of 20. Element states of the catalyst were acquired by X-ray photoelectron spectroscope (XPS, Thermo ESCALAB 250, Al K $\alpha$ ,  $h\nu = 1486.6$  eV) performed on an RBD-upgraded PHI-5000C

ESCA system. The magnetic property of the catalyst was measured with a vibrating sample magnetometer (VSM, Lakeshore 7300) from -8000 Oe to +8000 Oe at room temperature. Inductively coupled plasma atomic emission spectrometry (ICP, Shimadzu ICPS-7510) was employed to determine the actual content of the metallic elements. The nitrogen adsorption-desorption isotherm and BJH pore size distribution of the as-prepared  $\text{Ni}_{0.20}\text{Pd}_{0.05}/\text{CB}$  catalyst were measured by using a Micromeritics TriStar II3020 automated gas adsorption analyzer at 77 K.

### 2.4. General procedure for Suzuki-Miyaura coupling reaction

Typically, 2.75 mmol (1.1 equiv) of phenylboronic acid, 5.0 mmol (2 equiv) of base and controlled amount of catalyst (0.1 mol% Pd) were mixed with a solution of 40 mL of EtOH/H<sub>2</sub>O (v/v = 1/1). The mixture was sonicated for 5 min until uniformly dispersed, then 2.5 mmol (1 equiv) of aryl halide was added into the above suspension under vigorous stirring. When the reaction completed, the reaction mixture was extracted with ethyl acetate (4 × 30 mL) and the catalyst was separated by filtering. Then the organic layers were combined and dried over anhydrous  $\text{Na}_2\text{SO}_4$ , followed by rotary evaporation and vacuum drying to give a residue. The product yields were determined by high performance liquid chromatography (HPLC, Agilent 1260 Infinity, equipped with Eclipse XDB-C18 column) according to the standard curve based on biphenyl. As for aryl bromide derivatives, the yields of the products were determined by column chromatography. To investigate the cycling performance, the catalyst filtered should be first washed with ethyl acetate followed by ethanol and water to remove the adsorbed aryl halides. The recycled catalyst can be reused five times in succession.

## 3. Results and discussion

### 3.1. Morphology and characterization of catalysts

It can be clearly seen from the TEM images that the particle size of Ni-Pd ranges from 50 nm to 190 nm with an average diameter of 113.2 nm (Fig. 1(a) and (d)) and some agglomerates appear to be formed. In contrast, the well-dispersed nanoparticles in the  $\text{Ni}_{0.20}\text{Pd}_{0.05}/\text{CB}$  exhibit a narrower size distribution with a much smaller average size of 22.4 nm (Fig. 1(b) and (d)), resulting in larger active surface areas and better catalytic performances. As shown in Fig. 1(c), the HRTEM observation reveals that the interplanar spacings of 0.204 nm and 0.243 nm are corresponding to Ni (111) and (110) planes, respectively, while the lattice spacing of 0.230 nm may be assigned to the (111) plane of the fcc system of Pd. Moreover, it is noted that the Pd nanocrystals with a thickness of ~1.67 nm and a length of ~7.92 nm are intimately coupled with the Ni cores and the as-formed core-shell-like Ni-Pd nanoparticles are well dispersed on the CB surface with much smaller particle size and narrower size distribution as compared with that of unsupported ones. To further prove that the core-shell-like structure is formed, an AADF-STEM image was taken (Fig. S1). The elemental mapping image (Ni + Pd) reveals that the Ni core is partially surrounded by Pd nanoparticles.

Fig. 2 shows the X-ray diffraction (XRD) patterns of CB, Ni/CB and  $\text{Ni}_{0.20}\text{Pd}_{0.05}/\text{CB}$  catalysts. The broad and intense peak of carbon black at around 24.8° is due to the (002) plane reflection of carbon materials. While the peaks at 44.5°, 51.8° and 76.4° can be indexed as the (111), (200) and (220) planes of Ni, respectively, indicating the face-centered-cubic (fcc) structure of nickel nanoparticles with good crystallinity. After the replacement of Ni with Pd on the surface of Ni NPs, three additional peaks appeared at around 40.2°, 46.5° and 68.0° corresponding to the (111), (200) and (220) crystal

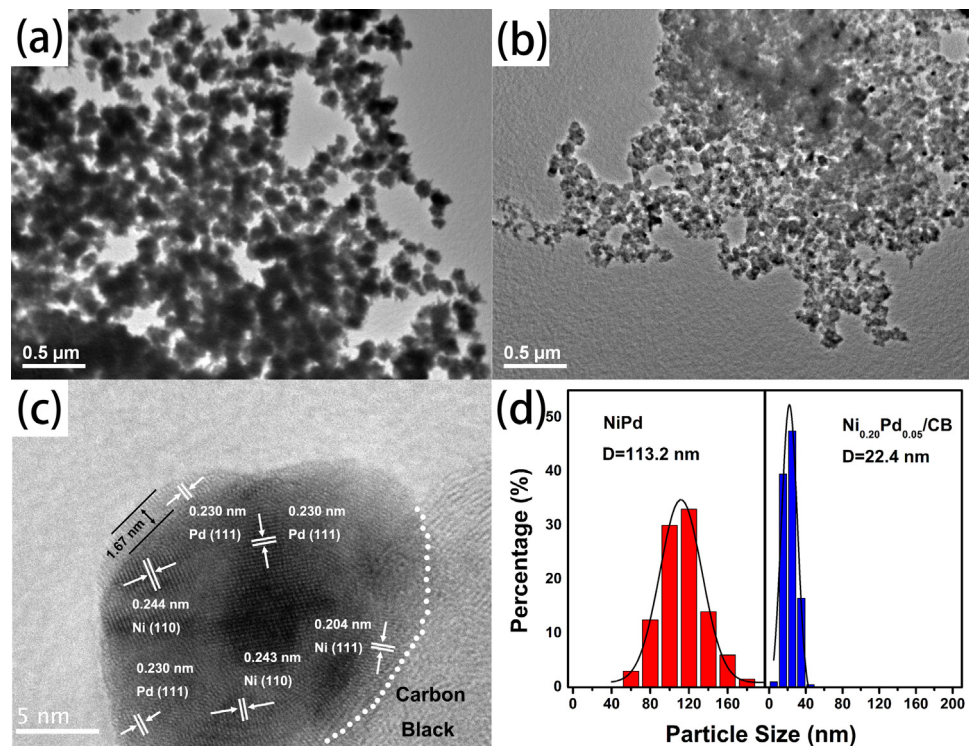


**Fig. 1.** (a,b) TEM images of Ni-Pd and  $\text{Ni}_{0.20}\text{Pd}_{0.05}/\text{CB}$  catalysts; (c) HRTEM image of  $\text{Ni}_{0.20}\text{Pd}_{0.05}/\text{CB}$  catalyst; (d) Particle size distributions of Ni-Pd and  $\text{Ni}_{0.20}\text{Pd}_{0.05}/\text{CB}$  catalysts.

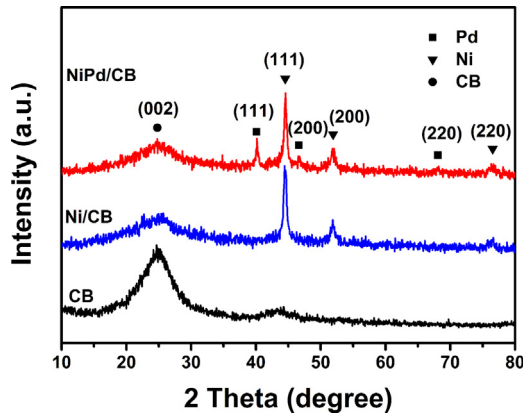


**Fig. 2.** XRD patterns of CB, Ni/CB and  $\text{Ni}_{0.20}\text{Pd}_{0.05}/\text{CB}$  catalyst.

planes of face-centered-cubic (fcc) Pd, suggesting the reduction of  $\text{Pd}^{2+}$  to  $\text{Pd}^0$ .

X-ray photoelectron spectroscopy (XPS) is one of powerful surface analysis technologies that measure the chemical composition, chemical state and electronic state of the elements. The global XPS spectra of Ni/CB and  $\text{Ni}_{0.20}\text{Pd}_{0.05}/\text{CB}$  catalysts (Fig. 3 (a)) show that Ni/CB contains C, O and Ni as the primary elements while in the  $\text{Ni}_{0.20}\text{Pd}_{0.05}/\text{CB}$  catalyst, peaks (330–355 eV) of Pd appear accompanying with the intensity decrease of Ni peaks (849–887 eV). The Ni/Pd atomic ratio was further determined to be 5.48 by ICP-AES, which is much higher than the value of 1.31 estimated by using the XPS result. Such a big difference in atomic ratio may be attributed to that the Pd element mainly distributes on the catalyst surface. Fig. 3(b) and (c) present the curve-fitted Ni 2p spectra of Ni/CB and  $\text{Ni}_{0.20}\text{Pd}_{0.05}/\text{CB}$ . The peak centered at 852.7 eV is ascribed to metallic Ni while two doublets located at 856.1 eV and 873.7 eV, 861.7 eV and 879.7 eV, may be assigned to  $\text{Ni}^{2+}$  in  $\text{NiO}$  and  $\text{Ni(OH)}_2$ , respectively. The existence of nickel oxide and hydroxide is due to

that the surface  $\text{Ni}^0$  atoms can easily suffer from oxidation when exposed to air, especially hydrous environment [34,35]. As shown in Fig. 3(e), the Pd 3d XPS spectrum can be deconvoluted into two sets of doublet components. The relatively lower binding energy set of doublet at 336.3 eV and 341.5 eV belongs to metallic Pd, while the other set of doublet at 338.2 eV and 343.5 eV is ascribed to the +2 oxidation state of Pd. As displayed in Fig. 3(d), the peaks centered at the binding energies of 284.6, 285.4, 286.6, 288.2 and 290.2 eV are corresponding to  $\text{sp}^2$  carbon,  $\text{sp}^3$  carbon, C–O, C=O species and  $\pi-\pi^*$  transition loss [36,37].

Fig. 4(a) shows the nitrogen adsorption-desorption isotherm and BJH pore size distribution of the as-prepared  $\text{Ni}_{0.20}\text{Pd}_{0.05}/\text{CB}$  catalyst. The values of BET surface area ( $S_{\text{BET}}$ ) and pore volume were  $120.12 \text{ cm}^2 \text{ g}^{-1}$  and  $0.26 \text{ cm}^3 \text{ g}^{-1}$ , respectively. Fig. 4(a) shows a typical IUPAC type IV pattern with a hysteresis loop, suggesting the existence of mesopores. Interestingly, the inset in Fig. 4(a) further reveals that they are dual-ordered mesopores of 3.72 and 33.04 nm. Large specific surface area and mesoporous structure are beneficial for the dispersion of NPs and the adsorption of organic molecules, leading to enhanced catalytic performance. The magnetic properties of the  $\text{Ni}_{0.20}\text{Pd}_{0.05}/\text{CB}$  catalyst was measured with a vibrating sample magnetometer (VSM, Lakeshore 7300) from  $-8000 \text{ Oe}$  to  $+8000 \text{ Oe}$  at room temperature. The typical hysteresis loop of the catalyst is shown in Fig. 4(b) with the saturation magnetization ( $M_s$ ), remanent magnetization ( $M_r$ ) and coercivity ( $H_c$ ) values of  $3.64 \text{ emu g}^{-1}$ ,  $1.03 \text{ emu g}^{-1}$  and  $208.5 \text{ Oe}$  (left insert of Fig. 4b), respectively, indicating the soft magnetic nature of the catalyst. The right inset of Fig. 4(b) shows that the catalyst can be separated easily from the reaction mixture by an external magnetic field.

### 3.2. Suzuki-Miyaura coupling reactions

The Ni-Pd/CB catalysts described above were applied to the SMC reaction of phenylboronic acid with aryl halides. The results of the SMC reaction of bromobenzene with phenylboronic acid are shown in Fig. 5. It can be clearly seen that there are signif-

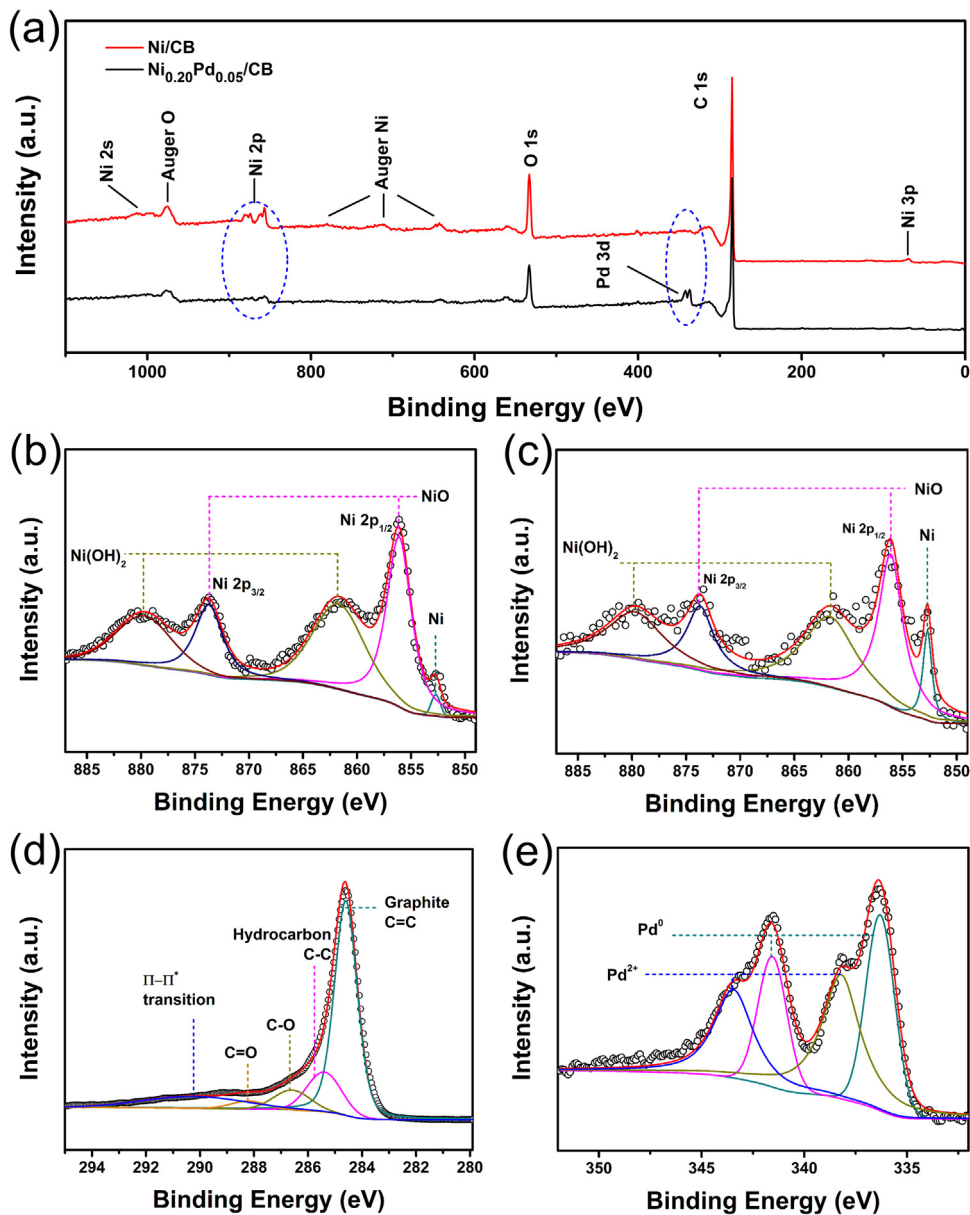


**Fig. 3.** (a) Global XPS spectra of Ni/CB and Ni<sub>0.20</sub>Pd<sub>0.05</sub>/CB catalysts; (b-e) Ni 2p, C 1s and Pd 3d of Ni<sub>0.20</sub>Pd<sub>0.05</sub>/CB core-level XPS spectra, respectively.

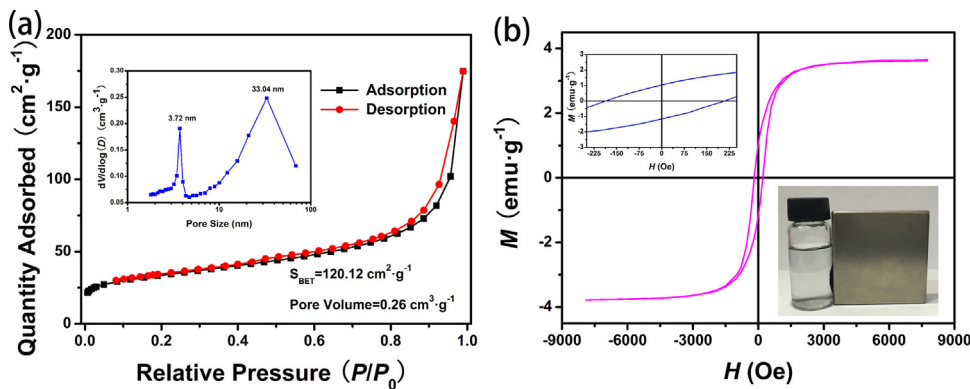


**Fig. 4.** (a) Nitrogen adsorption-desorption isotherm and BJH pore size distribution (inset) of the as-prepared Ni<sub>0.20</sub>Pd<sub>0.05</sub>/CB catalyst; (b) Magnetic hysteresis loop of Ni<sub>0.20</sub>Pd<sub>0.05</sub>/CB catalyst. The inserts show its magnetic hysteresis loop in low field zone (left) and magnetic separation effect (right).

icant differences in biphenyl yield among the various catalysts and the supported Ni-Pd/CB catalysts exhibit much better cat-

alytic performances than the unsupported ones. The Pd loading amount was fixed as low as 5 wt% and loading amount of Ni is con-

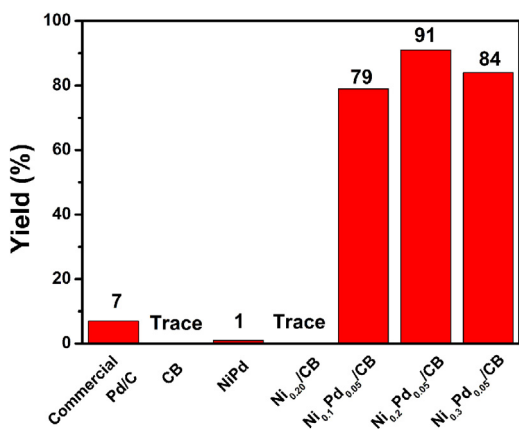


**Fig. 5.** Suzuki-Miyaura coupling reaction catalyzed by different catalysts. Reaction conditions: bromobenzene (2.5 mmol, 1 equiv), phenylboric acid (2.75 mmol, 1.1 equiv), base (5 mmol, 2 equiv), EtOH/H<sub>2</sub>O = 20 mL/20 mL, catalyst (5.5 mg, 0.1 mol% Pd if the catalyst contains Pd), 30 °C, 45 min. Yields were determined by HPLC according to the standard curve based on biphenyl.

**Table 1**

Effect of the temperature on the catalytic yields using  $\text{Ni}_{0.20}\text{Pd}_{0.05}/\text{CB}$  catalyst.

Entry	Temperature (°C)	Reaction time (min)	Yield (%)
1	30	20	51
2	30	60	>99
3	40	20	85
4	50	20	92
5	60	20	95

Reaction conditions: bromobenzene (2.5 mmol, 1 equiv), phenylboric acid (2.75 mmol, 1.1 equiv), Base (5 mmol, 2 equiv), EtOH/H<sub>2</sub>O = 20 mL/20 mL,  $\text{Ni}_{0.20}\text{Pd}_{0.05}/\text{CB}$  (5.5 mg, 0.1 mol% Pd).

Yields were determined by HPLC according to the standard curve based on biphenyl.

trolled less than 30 wt% to prevent aggregation (Fig. S2) [34]. Among the Ni-Pd/CB catalysts with different Ni/Pd ratio investigated,  $\text{Ni}_{0.20}\text{Pd}_{0.05}/\text{CB}$  gives the highest product yield over 91% within 45 min. The excellent activity of Ni-Pd/CB is mainly due to the synergistic effects of the individual components of the catalyst, which will be illustrated in detail later. Additionally, the SMC reaction follows the pseudo-second-order kinetics as shown in Fig. S3. The  $\text{Ni}_{0.20}\text{Pd}_{0.05}/\text{CB}$  gives a  $k_2$  value of 2.464 (mol L<sup>-1</sup>)<sup>-1</sup> min<sup>-1</sup>, which is higher than those of  $\text{Ni}_{0.10}\text{Pd}_{0.05}/\text{CB}$  and  $\text{Ni}_{0.30}\text{Pd}_{0.05}/\text{CB}$ . It is necessary to investigate whether the coupling reaction catalyzed by  $\text{Ni}_{0.20}\text{Pd}_{0.05}/\text{CB}$  or the leached homogeneous Pd species. A certain amount of  $\text{Ni}_{0.20}\text{Pd}_{0.05}/\text{CB}$  was firstly dispersed in EtOH/H<sub>2</sub>O/K<sub>2</sub>CO<sub>3</sub> system under ultrasound and then filtrated to obtain a transparent solution. After that, the corresponding amount of phenylboronic acid and bromobenzene were added into the solution with stirring and no biphenyl was detected even after 3 h. Moreover, the SMC reaction was carried out under mechanical and magnetic stirring, respectively. It is found that the magnetic property did not help to improve the catalytic activity.

**Table 1** shows the effect of the temperature on the SMC reaction yields using  $\text{Ni}_{0.20}\text{Pd}_{0.05}/\text{CB}$ . It is obvious that the product yield increases notably with increasing temperature (entries 1, 3–5) and the biphenyl can be obtained in over 85% yield within 20 min in the range of 30–60 °C. However, it should be noted that high yield (>99%) can also be achieved even at 30 °C just for a slightly longer time of 60 min (entry 2). Hence, choosing 30 °C as the SMC reaction temperature is in conformity with the principles of green chemistry.

It is known that bases can act as a bridge to connect bromobenzene and phenylboric acid, thus the nature of base is one of important factors in SMC reaction. Moreover, the surface organo-palladium species become an electrophilic intermediate in

**Table 2**  
Effect of different bases on the catalytic yields using  $\text{Ni}_{0.20}\text{Pd}_{0.05}/\text{CB}$  catalyst.

<chem>c1ccccc1Br</chem> + <chem>c1ccccc1B(O)O</chem> $\xrightarrow[\text{EtOH/H}_2\text{O (v/v=1/1)}]{\text{Ni}_{0.20}\text{Pd}_{0.05}/\text{CB}, \text{Base, } 30^\circ\text{C}}$		<chem>c1ccccc1-c2ccccc2</chem>
Entry	Base	Yield (%)
1	$\text{Cs}_2\text{CO}_3$	>99
2	$\text{K}_2\text{CO}_3$	>99
3	$\text{KHCO}_3$	81
4	$\text{Na}_2\text{CO}_3$	99
5	$\text{NaHCO}_3$	11
6	$\text{Na}_3\text{PO}_4 \cdot 12\text{H}_2\text{O}$	98
7	$^t\text{BuOK}$	99
8	$\text{MeONa}$	57
9	$\text{Et}_3\text{N}$	8
10	CHA	Trace

Reaction conditions: bromobenzene (2.5 mmol, 1 equiv), phenylboric acid (2.75 mmol, 1.1 equiv), Base (5 mmol, 2 equiv), EtOH/H<sub>2</sub>O = 20 mL/20 mL,  $\text{Ni}_{0.20}\text{Pd}_{0.05}/\text{CB}$  (5.5 mg, 0.1 mol% Pd), 30 °C, 1 h.

Yields were determined by HPLC according to the standard curve based on biphenyl.

**Table 3**

Effect of different solvents on the catalytic yields using  $\text{Ni}_{0.20}\text{Pd}_{0.05}/\text{CB}$  catalyst.

<chem>c1ccccc1Br</chem> + <chem>c1ccccc1B(O)O</chem> $\xrightarrow[\text{Solvent}]{\text{Ni}_{0.20}\text{Pd}_{0.05}/\text{CB}, \text{K}_2\text{CO}_3, 30^\circ\text{C}}$		<chem>c1ccccc1-c2ccccc2</chem>
Entry	Solvent (mL/mL)	Yield (%)
1	$\text{CCl}_4 = 40$	Trace
2	$\text{DMF} = 40$	Trace
3	$\text{DMSO} = 40$	Trace
4	$\text{MeOH} = 40$	4
5	$\text{EtOH} = 40$	56
6	$\text{IPA} = 40$	2
7	$\text{H}_2\text{O} = 40$	14
8	$\text{DMF/H}_2\text{O} = 20/20$	25
9	$\text{DMSO/H}_2\text{O} = 20/20$	28
10	$\text{MeOH/H}_2\text{O} = 20/20$	17
11	$\text{EtOH/H}_2\text{O} = 20/20$	>99
12	$\text{IPA/H}_2\text{O} = 20/20$	78

Reaction conditions: bromobenzene (2.5 mmol, 1 equiv), phenylboric acid (2.75 mmol, 1.1 equiv),  $\text{K}_2\text{CO}_3$  (5 mmol, 2 equiv), EtOH/H<sub>2</sub>O = 20 mL/20 mL,  $\text{Ni}_{0.20}\text{Pd}_{0.05}/\text{CB}$  (5.5 mg, 0.1 mol% Pd), 30 °C, 1 h.

Yields were determined by HPLC according to the standard curve based on biphenyl.

an alkaline environment, meanwhile dissolving boranate complex forms, thus greatly affecting the subsequent transmetalation process [38]. Various bases, such as  $\text{Cs}_2\text{CO}_3$ ,  $\text{K}_2\text{CO}_3$ ,  $\text{KHCO}_3$ ,  $\text{Na}_2\text{CO}_3$ ,  $\text{NaHCO}_3$ ,  $\text{Na}_3\text{PO}_4 \cdot 12\text{H}_2\text{O}$ ,  $^t\text{BuOK}$ ,  $\text{MeONa}$ ,  $\text{Et}_3\text{N}$  and cyclohexylamine (CHA) were employed in SMC reaction under the same conditions, and the results are listed in **Table 2**. Among these bases,  $\text{Cs}_2\text{CO}_3$ ,  $\text{K}_2\text{CO}_3$ ,  $\text{Na}_2\text{CO}_3$  and  $\text{Na}_3\text{PO}_4$  behave as very efficient bases for SMC reaction in EtOH/H<sub>2</sub>O system with over 98% yield of biphenyl (entries 1, 2, 4, 6). However, the other inorganic bases, such as  $\text{KHCO}_3$  and  $\text{NaHCO}_3$ , only gave lower yields in the reaction (entries 3, 5). As for the organic bases,  $^t\text{BuOK}$  behaves as the very powerful base in the reaction with the yield up to 99% (entry 7), while the others exhibited extremely poor biphenyl yields (entries 8–10). It should be pointed out that the choice of base still depends on empirical findings, so that a general rule for their selection is needed urgently to be established. In view of the cost and availability of the bases tested in this work,  $\text{K}_2\text{CO}_3$  can be considered as the most appropriate choice.

As can be seen from **Table 3**, the nature of solvent also has an important influence on the biphenol yields in SMC reaction. It is obvious that there is almost no product in aprotic solvents such as  $\text{CCl}_4$ , DMF and DMSO (entries 1–3), while relatively higher yields can be achieved when using protic solvents (entries 4–7). Interestingly, mixed water-organic solvent can tremendously increase

the biphenyl yield (entries 8–12), especially the EtOH/H<sub>2</sub>O system (v/v = 1/1, entry 10) gives a yield as high as 99%. Such an improvement may be attributed to two factors: (1) the mixed EtOH/H<sub>2</sub>O system is suitable for the dissolution of bases and organic reactants, thus facilitating the formation of boronate complex and the interaction between the catalysts and reactants [38], (2) biphenyl, as the product with acceptable solubility, will precipitate during the reaction process, driving the equilibrium beneficial to produc-

tion generation [20]. Compared with other solvents studied in this work, the EtOH/H<sub>2</sub>O (v/v = 1/1) system shows the following advantages: high efficiency, environmentally friendly property and easy post-process.

Generality of Ni<sub>0.20</sub>Pd<sub>0.05</sub>/CB catalyst in SMC reaction was investigated by using different substituent aryl bromides containing electron-donating and electron-withdrawing functional groups under optimized conditions (Table 4). The biphenyl

**Table 4**

Generality of Ni<sub>0.20</sub>Pd<sub>0.05</sub>/CB catalyst in Suzuki-Miyaura coupling reaction involving different aryl halides under stated reaction conditions.

Entry	Aryl halide	Temperature (°C)	Time	Product	Yield (%)
				EtOH/H <sub>2</sub> O (v/v=1/1)	
1		30	3 h		5
2		30	45 min		91
3		30	30 min		90
4		80	10 h		17
5		80	10 h		34
6		80	10 h		60
7		80	10 h		28
8		80	10 h		47
9		30	45 min		79
10		30	45 min		86
11		30	45 min		94
12		30	45 min		88
13		30	45 min		88
14		30	45 min		92
15		30	45 min		90
16		30	45 min		95
17		30	30 min		86
18		30	30 min		92
19		60	90 min		89
20		60	60 min		89

Reaction conditions: aryl halide (2.5 mmol, 1 equiv), phenylboric acid (2.75 mmol, 1.1 equiv), K<sub>2</sub>CO<sub>3</sub> (5 mmol, 2 equiv), EtOH/H<sub>2</sub>O = 20 mL/20 mL, Ni<sub>0.20</sub>Pd<sub>0.05</sub>/CB (5.5 mg, 0.1 mol% Pd).

Isolated yields.

yields of different halobenzenes follow the order of iodobenzene > bromobenzene ≫ chlorobenzene (entries 1–3) due to the difference in electronegativity of individual halogen elements. It is well known that the order of halogen electronegativity is Cl (3.16) > Br (2.96) > I (2.66). The higher electronegativity gives stronger strength of carbon-halogen bond, thus resulting in lower biphenyl yields [19,39]. Hence, aryl halides can give fairish yields of corresponding products under strict conditions, such as 80 °C and 10 h (entries 4–8). As for the OMe-substituted bromobenzene, *p*-substituted-OMe gives the highest yield of 94%, while *o*-NO<sub>2</sub>-substituted chlorobenzene (entries 4–6) and *o*-substituted-OMe (entries 9–11) give lower yields owing to the steric hindrance [38]. Moreover, the catalyst is also applicable for other para-substituent aryl bromides, such as *p*-Me, *p*-CN, *p*-NO<sub>2</sub>, etc. (entries 12–16). As for meta-substituent aryl iodides, higher yields can be obtained even within a short time of 30 min (entries 17–18). In addition, coupling of 1-bromonaphthalene and arylboronic acid also can give a yield as high as 89% under the condition of higher reaction temperature and prolonged time (entry 19), while for 1-iodonaphthalene, a high yield can also be achieved in a shorter time (entry 20) due to the weaker C—I bond. The catalytic activity of Ni<sub>0.20</sub>Pd<sub>0.05</sub>/CB is superior to the results reported in literatures [39–43].

Stable reusability was one of the most important properties of one catalyst. The as-prepared Ni<sub>0.20</sub>Pd<sub>0.05</sub>/CB catalyst was tested over 5 times under optimized conditions in succession. As shown in Fig. 6, Ni<sub>0.20</sub>Pd<sub>0.05</sub>/CB exhibited relatively excellent cycling performance with the product yield of over 80% after 5 cycles. The metal amount in unused Ni<sub>0.20</sub>Pd<sub>0.05</sub>/CB was 14.43 wt% of Ni and 4.78 wt% of Pd, respectively, while in the reused catalyst, the value become 10.98 wt% of Ni and 3.52 wt% of Pd, respectively, which is one reason of the decrease in catalytic activity. Additionally, structure of reused Ni<sub>0.20</sub>Pd<sub>0.05</sub>/CB catalyst was characterized by TEM and XPS. The TEM images (Fig. S4(a)) show that agglomeration of nanoparticles appears after the 5th cycle, meanwhile, a small amount of Pd nanoparticles flaked off from the surface of Ni core onto the surface of carbon black (Fig. S4(b–c)). And it can be concluded by XPS analysis that the aerobic reaction condition may cause the reused catalyst to decrease in Ni<sup>0</sup> and increase in Pd<sup>2+</sup> compared with the

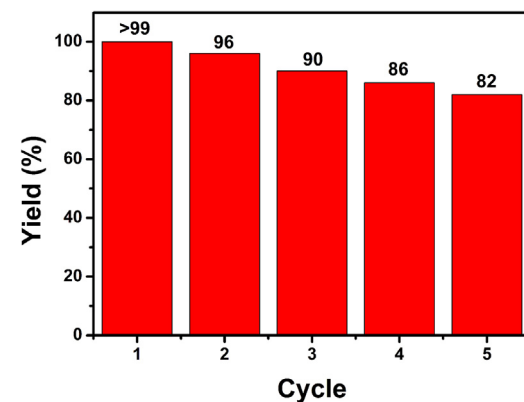


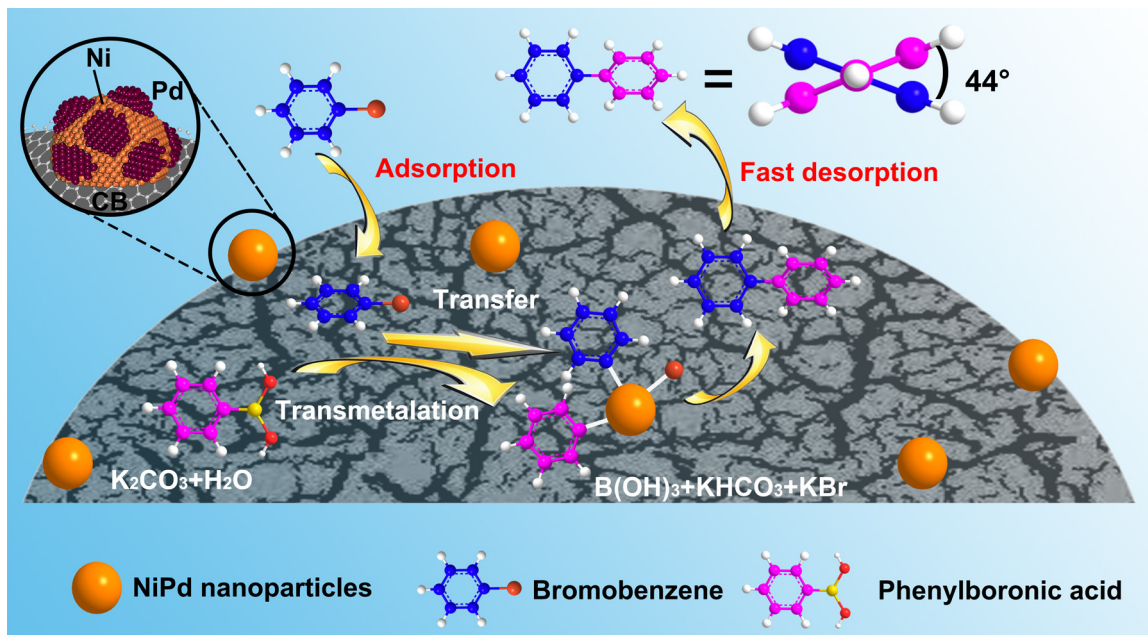
**Fig. 6.** Cycling performance of Ni<sub>0.20</sub>Pd<sub>0.05</sub>/CB in Suzuki-Miyaura coupling reaction.

unused one, leading to the decreased catalytic performance (Fig. S5).

#### 4. Insight into the reaction mechanism

**Scheme 1** illustrates a proposed plausible reaction mechanism by taking coupling of bromobenzene with phenylboronic acid as an instance. The absorbed bromobenzene molecules on the CB surface can easily gain access to Ni-Pd nanoparticles to form surface organo-palladium species via the oxidative addition. In presence of bases, the surface organo-palladium species become an electrophilic intermediate, followed by transmetalation with the generation of B(OH)<sub>3</sub>, KHCO<sub>3</sub> and KBr [2,20,44,45]. Afterwards, the reaction is completed and the desired biphenyl is obtained by means of reductive elimination, accompanying the catalyst restoration.

The high catalytic performance of Ni<sub>0.20</sub>Pd<sub>0.05</sub>/CB catalyst can be attributed to its hybrid nanostructure and the synergistic effects between the individual components. Firstly, the high specific surface area of CB is not only beneficial for the dispersion and stability of Ni-Pd nanoparticles, but also propitious to the rapid diffusion of reactants. It is noted that there exists the π-π stacking interac-



**Scheme 1.** Possible mechanism of Suzuki-Miyaura coupling reaction catalyzed by Ni<sub>0.20</sub>Pd<sub>0.05</sub>/CB.

tion between carbon black and aromatic bromobenzene molecules, which helps in gaining easier access of the reactants to Ni-Pd nanoparticles [46,47]. On the other hand, non-coplanar of two benzene rings in aromatic biphenyl also accelerates the reaction by forcing product molecules away from the surface of carbon black [48]. Secondly, compared with Pd nanoparticle alone, the unique core-shell-like Ni-Pd nanostructure can greatly improve the utility of Pd element while the inner Ni particle core has a strong magnetic property, which makes the  $\text{Ni}_{0.20}\text{Pd}_{0.05}/\text{CB}$  catalyst magnetically separable in a suspension system, thus the introduction of additional magnetic component is no longer necessary as is the usual case. Thirdly, steric configuration of biphenyl and its solubility in EtOH/H<sub>2</sub>O system further facilitate the reaction process. Moreover, the precipitation of biphenyl during the reaction process can drive the equilibrium to the product side. In account of polarity, the adsorption process takes place more easily between hydrophilic sheet and polarized substrates, especially for the phenylboronic acid molecules, while the less polarized biphenyl readily dissociates and further facilitates the product generation [49].

## 5. Conclusions

In summary, a magnetically separable core-shell-like Ni-Pd/CB catalyst was designed and successfully fabricated via a facile sequential reduction approach. TEM observation showed that the Pd nanocrystals were intimately coupled with the Ni cores and the resulting core-shell-like Ni-Pd nanoparticles were highly dispersed on the surface CB with much smaller particle size and narrower size distribution as compared with that of unsupported Ni-Pd nanoparticles. The catalyst exhibited high performance in Suzuki–Miyaura coupling reactions in air under mild conditions without using toxic solvents, ligands or protective atmosphere, achieving green and efficient catalysis. The high catalytic performance of Ni-Pd/CB catalyst can be attributed to its unique core-shell-like nanostructure and the synergistic effects between the individual components, mainly including (1) high specific surface area of CB and its porous structure are beneficial for the dispersion and stability of Ni-Pd nanoparticles and the rapid diffusion of reactants; (2) the  $\pi$ - $\pi$  stacking interaction between carbon black and aromatic bromobenzene molecules helps in gaining easier access of the reactants to Ni-Pd nanoparticles; (3) the smaller-sized Pd nanocrystals on Ni cores can provide more reaction centers; (4) the presence of Ni component can make the catalyst magnetically separable in a suspension system and effectively lower the cost. Overall, such a low-cost and high-performance nanocatalyst may bring new design opportunities for C–C coupling catalysis on an industrial scale in the future.

## Acknowledgements

This work was supported by NSF of China (No. 51572125), China Postdoctoral Science Foundation (No. 2014M561651, No. 2015T80554), Jiangsu Planned Projects for Postdoctoral Research Funds (No. 1401003B), the Fundamental Research Funds for the Central Universities (No. 20915011311, No. 30916014103) and PAPD of Jiangsu.

## Appendix A. Supplementary data

Supplementary data associated with this article can be found, in the online version, at <http://dx.doi.org/10.1016/j.apcatb.2016.06.066>.

## References

- [1] H. Li, C.C. Johansson Seechurn, T.J. Colacot, *ACS Catal.* 2 (2012) 1147–1164.
- [2] B.A. Khakiani, K. Pourshamsian, H. Veisi, *Appl. Organomet. Chem.* 29 (2015) 259–265.
- [3] I. Maluenda, O. Navarro, *Molecules* 20 (2015) 7528–7557.
- [4] A. Chatterjee, H. Mallin, J. Klehr, J. Vallaparakkal, A. Finke, L. Vera, M. Marsh, T. Ward, *Synfacts* 12 (2016), 0317–0317.
- [5] E. Mieczyńska, J. Lisowski, A.M. Trzeciak, *Inorg. Chim. Acta* 431 (2015) 145–149.
- [6] M. Gholinejad, M. Razeghi, C. Najera, *RSC Adv.* 5 (2015) 49568–49576.
- [7] R. Martin, S.L. Buchwald, *Acc. Chem. Res.* 41 (2008) 1461–1473.
- [8] R. Jana, T.P. Pathak, M.S. Sigman, *Chem. Rev.* 111 (2011) 1417–1492.
- [9] H.A. Elazab, A.R. Sihamaki, S. Moussa, B.F. Gupton, M.S. El-Shall, *Appl. Catal. A* 491 (2015) 58–69.
- [10] M.C. Hong, H. Ahn, M.C. Choi, Y. Lee, J. Kim, H. Rhee, *Appl. Organomet. Chem.* 28 (2014) 156–161.
- [11] B. Jiang, S. Song, J. Wang, Y. Xie, W. Chu, H. Li, H. Xu, C. Tian, H. Fu, *Nano Res.* 7 (2014) 1280–1290.
- [12] M. Kim, J.C. Park, A. Kim, K.H. Park, H. Song, *Langmuir* 28 (2012) 6441–6447.
- [13] P. Wang, G. Zhang, L. Liu, H. Jiao, X. Deng, X. Zheng, *Mater. Res. Bull.* 59 (2014) 365–369.
- [14] A. Ohtaka, J.M. Sansano, C. Nájera, I. Miguel-García, Á. Berenguer-Murcia, D. Cazorla-Amorós, *ChemCatChem* 7 (2015) 1841–1847.
- [15] C. Feng, J. Liu, J. Gui, L. Liu, Chin. J. Appl. Chem. 32 (2015) 19–26.
- [16] V. Polshettiwar, A. Decottignies, C. Len, A. Fihri, *ChemSusChem* 3 (2010) 502–522.
- [17] A. Balanta, C. Godard, C. Claver, *Chem. Soc. Rev.* 40 (2011) 4973–4985.
- [18] M.L. Chtchigrovsky, Y. Lin, K. Ouchau, M. Chaumontet, M. Robitzer, F. Quignard, F. Taras, *Chem. Mater.* 24 (2012) 1505–1510.
- [19] L. Zhang, C. Feng, S. Gao, Z. Wang, C. Wang, *Catal. Commun.* 61 (2015) 21–25.
- [20] J. Sun, Y. Fu, G. He, X. Sun, X. Wang, *Appl. Catal. B* 165 (2015) 661–667.
- [21] M. Gholinejad, M. Seyedhamzeh, M. Razeghi, C. Najera, M. Kompany-Zareh, *ChemCatChem* 8 (2016) 441–447.
- [22] Y. She, Z. Lu, W. Fan, S. Jewell, M.K. Leung, *J. Mater. Chem. A* 2 (2014) 3894–3898.
- [23] Y. Wu, D. Wang, P. Zhao, Z. Niu, Q. Peng, Y. Li, *Inorg. Chem.* 50 (2011) 2046–2048.
- [24] Q. Guo, D. Liu, X. Zhang, L. Li, H. Hou, O. Niwa, T. You, *Anal. Chem.* 86 (2014) 5898–5905.
- [25] Ö. Metin, S.F. Ho, C. Alp, H. Can, M.N. Mankin, M.S. Gültkin, M. Chi, S. Sun, *Nano Res.* 6 (2013) 10–18.
- [26] J. Xiang, P. Li, H. Chong, L. Feng, F. Fu, Z. Wang, S. Zhang, M. Zhu, *Nano Res.* 7 (2014) 1337–1343.
- [27] L. Feng, H. Chong, P. Li, J. Xiang, F. Fu, S. Yang, H. Yu, H. Sheng, M. Zhu, *J. Phys. Chem. C* 119 (2015) 11511–11515.
- [28] S. Hung, Y. Yu, N. Suen, G. Tzeng, C. Tung, Y. Hsu, C. Hsu, C. Chang, T. Chan, H. Sheu, *Chem. Commun.* 52 (2016) 1567–1570.
- [29] R.K. Rai, K. Gupta, D. Tyagi, A. Mahata, S. Behrens, X. Yang, Q. Xu, B. Pathak, S.K. Singh, *Catal. Sci. Technol.* (2016).
- [30] R.K. Rai, K. Gupta, S. Behrens, J. Li, Q. Xu, S.K. Singh, *ChemCatChem* 7 (2015) 1806–1812.
- [31] M. Xiao, J. Zhu, J. Ge, C. Liu, W. Xing, *J. Power Sources* 281 (2015) 34–43.
- [32] H. He, M. Zhong, D. Konkolewicz, K. Yacatto, T. Rappold, G. Sugar, N.E. David, K. Matyjaszewski, *J. Mater. Chem. A* 1 (2013) 6810–6821.
- [33] Y. Hoshikawa, B. An, S. Kashihara, T. Ishii, M. Ando, S. Fujisawa, K. Hayakawa, S. Hamatani, H. Yamada, T. Kyotani, *Carbon* 99 (2016) 148–156.
- [34] J. Xia, G. He, L. Zhang, X. Sun, X. Wang, *Appl. Catal. B* 180 (2016) 408–415.
- [35] W. Lin, H. Cheng, J. Ming, Y. Yu, F. Zhao, *J. Catal.* 291 (2012) 149–154.
- [36] H. Estrade-Szwarcopf, *Carbon* 42 (2004) 1713–1721.
- [37] H. Qian, H. Huang, X. Wang, *J. Power Sources* 275 (2015) 734–741.
- [38] H. Song, Q. Zhu, X. Zheng, X. Chen, *J. Mater. Chem. A* 3 (2015) 10368–10377.
- [39] D. Dumbré, P. Yadav, S. Bhargava, V. Choudhary, *J. Catal.* 301 (2013) 134–140.
- [40] X. Le, Z. Dong, Y. Liu, Z. Jin, T. Do Huy, M. Le, J. Ma, *J. Mater. Chem. A* 2 (2014) 19696–19706.
- [41] C. Deraedt, L. Salmon, L. Etienne, J. Ruiz, D. Astruc, *Chem. Commun.* 49 (2013) 8169–8171.
- [42] M. Gholinejad, M. Razeghi, A. Ghaderi, P. Bijji, *Catal. Sci. Technol.* 6 (2016) 3117–3127.
- [43] A. Fihri, D. Cha, M. Bouhrara, N. Almana, V. Polshettiwar, *ChemSusChem* 5 (2012) 85–89.
- [44] F. Han, *Chem. Soc. Rev.* 42 (2013) 5270–5298.
- [45] A. Fihri, M. Bouhrara, B. Nekoueishahraki, J.M. Basset, V. Polshettiwar, *Chem. Soc. Rev.* 40 (2011) 5181–5203.
- [46] F. Cozzi, M. Cinquini, R. Annuziata, J.S. Siegel, *J. Am. Chem. Soc.* 115 (1993) 5330–5331.
- [47] Q. Liu, T. Zheng, P. Wang, J. ?P. Jiang, N. Li, *Chem. Eng. J.* 157 (2010) 348–356.
- [48] R. Nie, J. Shi, W. Du, Z. Hou, *Appl. Catal. A* 473 (2014) 1–6.
- [49] S. Yamamoto, H. Kinoshita, H. Hashimoto, Y. Nishina, *Nanoscale* 6 (2014) 6501–6505.